Structural health monitoring sensor development
for the Imote2 platform

Jennifer A. Rice*[a] and B.F. Spencer, Jr.[a]

[a] Dept. of Civil and Environmental Engineering, University of Illinois at Urbana-Champaign
205 N. Mathews Ave, Urbana, IL USA, 61801

ABSTRACT

The declining state of civil infrastructure has motivated researchers to seek effective methods for real-time structural health monitoring (SHM). Decentralized computing and data aggregation employing *smart sensors* allow the deployment of a dense array of sensors throughout a structure. The Imote2, developed by Intel, provides enhanced computation and communication resources that allow demanding sensor network applications, such as SHM of civil infrastructure, to be supported. This study explores the development of a versatile Imote2 sensor board with onboard signal processing specifically designed for the demands of SHM applications. The components of the accelerometer board have been carefully selected to allow for the low-noise and high resolution data acquisition that is necessary to successfully implement SHM algorithms.

Keywords: Structural health monitoring, smart sensor, wireless sensor.

1. INTRODUCTION

The growing decline of civil infrastructure in industrialized nations has caused increased interest and research in the area of structural health monitoring. Current inspection and maintenance practices are not adequate to ensure that structural damage is identified prior to catastrophic failure. The ability to gain real-time and pertinent information about the condition of a structure has the potential to increase public safety while decreasing the cost associated with the repair of extreme damage. The evolution of structural health monitoring research has seen a shift away from traditional wired monitoring schemes, which rely on a centralized data acquisition and processing, towards the use of wireless smart sensor networks. Such smart sensors allow much of the computational burden involved in effective SHM to be carried out by the sensor nodes themselves, thereby optimizing network resources by limiting the amount of RF communication that is required.

A smart sensor is defined by several key features which set it apart from traditional sensors. The first and most important feature is that a smart sensor must possess onboard computational ability by means of a microprocessor. This feature allows the smart sensor to act in a somewhat autonomous manner and to process data and implement SHM algorithms. The second feature is that the smart sensor must have the ability to store sensed data prior to processing and store process instructions and numerical algorithms in onboard memory. The third feature of a smart sensor is that it is wireless from both a data-acquisition perspective and from a power supply perspective. The wireless feature of a smart sensor requires that the node is either self-powered or battery powered and has an onboard radio. The final feature of a smart sensor is that it should be relatively low-cost so that a network of sensor nodes does not become prohibitively expensive as the node number increases.[1] Each of these features helps to ensure that a network of such sensors is scalable to a large number nodes – a requirement of the next generation of SHM systems for large civil structures.

The selection of an appropriate smart sensor platform must take into consideration the specific and demanding requirements of structural monitoring. There are many challenges associated with SHM that can be managed or eliminated when appropriate measures are taken in the design of the network, the sensor node, and the algorithms. One challenge of SHM is that it requires high sample rates and the use of computationally intense algorithms. Vibration-based SHM schemes call for signals from the sensors within the network to be carefully synchronized to accurately assess the structural condition.[2]

Intel's Imote2 provides a commercially available wireless sensor platform that possesses the elements required for data intensive applications such as SHM.[3] Previous wireless sensor platforms, such as the Mica Mote,[2] have focused on ultra low power performance and low data-rates. Although the Imote2 platform is well suited to high bit-rate applications, it does not have inherent sensing capabilities. Two options for sensing are currently available for the Imote2: (i) commercially available sensor board designed to interface with the Imote2,[5] or (ii) custom-developed sensor boards.

This paper reviews previous work done to characterize the performance of Intel's *Basic Sensor Board* and demonstrates the need for a more flexible sensor board designed specifically for SHM applications. The design and testing of a newly developed Structural Health Monitoring Accelerometer (SHM-A) board that interfaces with the Imote2 wireless sensor platform is presented and experimentally verified. The components of the sensor board have been selected to meet the requirements of vibration-based SHM applications, specifically with respect to data quality and the demands of achieving synchronized sensing.

2. IMOTE2 PLATFORM AND BASIC SENSOR BOARD

2.1 Imote2 features

The Imote2 (Figure 1), developed by Intel, is a wireless sensor platform that is well-suited to the demands of SHM applications. It has a low-power X-scale processor (PXA27x) with variable processing speed to optimize power consumption. It incorporates a ChipCon 2420 802.15.4 radio with an onboard antenna (Antenova Mica SMD). The onboard memory of the Imote2 is the feature that sets it apart from other wireless sensor platforms and allows its use for the high-frequency sampling required for dynamic structural monitoring. It has 256 KB of integrated RAM, 32 MB of external SDRAM, and 32 MB of flash memory.[6] Table 1 summarizes the features of the Imote2.
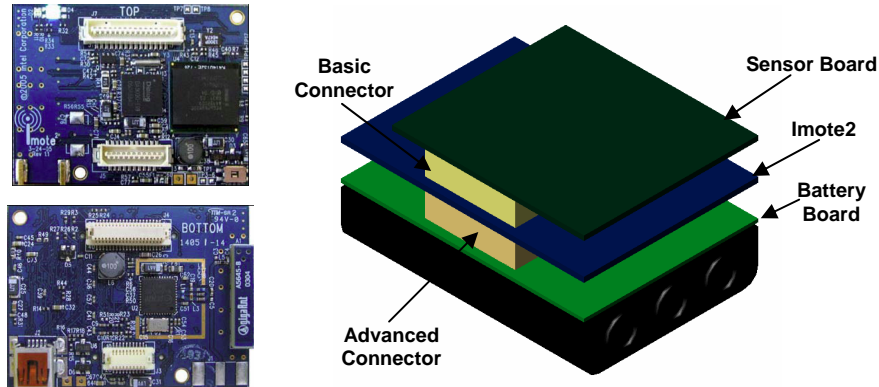

Figure 1. Top and bottom of Imote2 main board (left) and representation of Imote2 stackable configuration (right).

Table 1. Imote2 features.[6]

Feature	Value
Clock speed (MHz)	13-416
Active Power (mW)	44 @ 13 MHz, 570 @ 416 MHz
Program flash (bytes)	32 M
Data Rate (kbps)	250
RAM (bytes)	256 K + 32 M external
Nonvolatile storage (bytes)	32 M (Program flash)
Size (mm)	48 x 36 x 7

The Imote2 does not possess intrinsic sensing capabilities, but rather provides a flexible platform for a range of sensing applications. The sensors used with the Imote2 are interfaced to the main board via two connectors in a stackable configuration (see Figure 1). The Imote2 does not have an onboard analog-to-digital converter (ADC) and therefore is only compatible with digital sensor output. The options available for I/O are I2C (which allows interface to an unlimited number of channels), 3 SPI ports (serial data ports limited to one channel per port), and multiple GPIO (general purpose I/O) pins.[6]

TinyOS is the operating system used on the Imote2. Its small memory footprint is suited to the limited resources of smart sensors. TinyOS has a large user community and many successful smart sensor applications. However, some features of TinyOS pose limitations for SHM applications. Primarily, it does not support real time operations and thus has only two types of execution threads: 1) tasks and 2) hardware event handlers. This concurrency model leaves only a small amount of control to the user in the assignment of priority to commands; execution timing cannot be arbitrarily controlled. This limitation of TinyOS must be carefully considered when designing an SHM implementation.[7],[8]

2.2 Intel's *Basic Sensor Board*

One option for sensing with the Imote2 is to utilize a sensor board developed by Intel, now available from Crossbow. This *Basic Sensor Board* (ITS400) has a 3-axis digital accelerometer (ST Microelectronics LIS3L02DQ), a light sensor (TSL2561), and a temperature and relative humidity sensor (SHT15). The most recent board also incorporates a 4-channel, 12-bit ADC (Maxim 1363) and an additional temperature sensor (TMP175).[5] The performance of the LIS3L02DQ accelerometer on the original version of the *Basic Sensor Board* was evaluated by Nagamaya, et. al.[7] Some limitations of the *Basic Sensor Board* in the context of SHM applications were identified and will be discussed herein.

Table 2: LIS3L02DQ user specified sampling rates and cutoff frequencies.[9]

Decimation factor	Cutoff frequency (Hz)	Sampling rate (Hz)
128	70	280
64	140	560
32	280	1120
8	1120	4480

One drawback of the *Basic Sensor Board* for SHM applications is its lack of flexibility in selecting the cutoff frequency and sampling rate for data acquisition. The LIS3L02DQ has a built in ADC with digital filters with four selectable cutoff frequencies and corresponding sampling rate options which are selected by setting a decimation factor as shown in Table 2.[9] The specifications for the accelerometer state that when one of the given decimation factors is specified, the cutoff frequency and the sampling rate will be within 10 percent of the selected values.[10]

Another critical limitation of the *Basic Sensor Board* is that the accelerometer can have significant sampling rate errors. Tests revealed that the sampling rate did indeed vary from sensor to sensor even when the same decimation factor was selected. On a group of 14 sensor boards tested, the sampling rate varied from 537 to 605 Hz when a 560 Hz sample rate was selected. Although these results are within the manufacturers specifications, the variation undermines efforts to achieve the synchronized sensing which is critical for SHM applications. Additionally, tests showed that the sample rate on a given sensor was not constant in time, fluctuating up to 0.1%. This sample-rate fluctuation is attributed to the accelerometer and not the processor on the Imote2. Nagayama, et. al. [7] was able to achieve synchronized sensing with the *Basic Sensor Board* through the use of a resampling algorithm which involved timestamping the measured data. Although this approach was effective, it requires additional computation that drains the resources of the sensor node.

3. SENSOR BOARD DEVELOPMENT

3.1 Design criteria

A new Imote2 sensor board has been designed that provides flexible and accurate user-selectable sampling rates and anti-aliasing filtering capabilities. Because of the local nature of structural damage, higher mode responses of the structure are often required (up to 500 Hz) in addition to low-frequency signals (DC to 20 Hz). To avoid potential signal errors, especially in the higher frequency range, avoiding sample-rate fluctuation (jitter) is critical. While simply interfacing an analog accelerometer with a high-quality ADC could address the sampling rate issues, a programmable signal conditioner was chosen because of the flexibility it provides the user in terms of anti-aliasing and signal processing.

Vibration-based SHM requires the ability to measure small-amplitude structural vibration; therefore, sensors employed in such applications must possess appropriate sensitivity and noise characteristics. Several factors contribute to the quality of the measured digital signal that the sensor board outputs. The first is the sensitivity of the sensor, which is defined by the relationship between the physical phenomena that is sensed and the output of the sensor. The second factor is the noise floor of the sensor and other electrical components. The final factor is the resolution at which the analog signal is digitized by the ADC, which dictates the smallest measurable increment which can be quantified.

The key component of the Structural Health Monitoring Accelerometer (SHM-A) board described herein is the Quickfilter QF4A512, a versatile, 4-channel ADC and programmable signal conditioner with user-selectable sampling rates and programmable digital filters. The board interfaces with the Imote2 via SPI I/O and has a 3-axis analog accelerometer for vibration measurement. A block diagram of the components of the SHM-A sensor board is given in Figure 2. Figure 3 shows three views of the board. The details of each component will be discussed in subsequent sections.
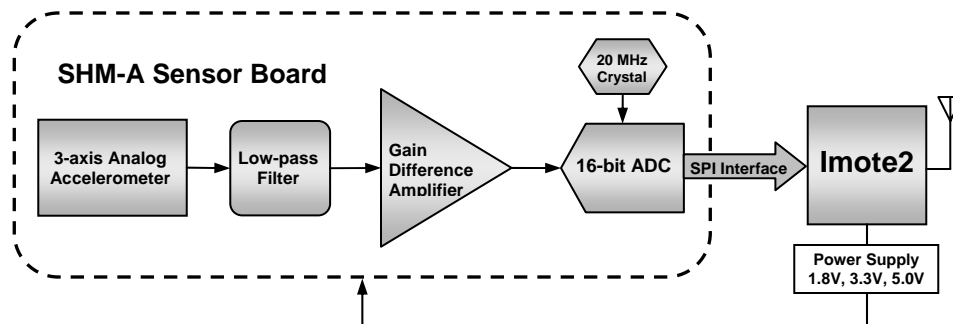

Figure 2. Block diagram of SHM-A sensor board (left) SHM-A board stacked on Imote2 and battery board.
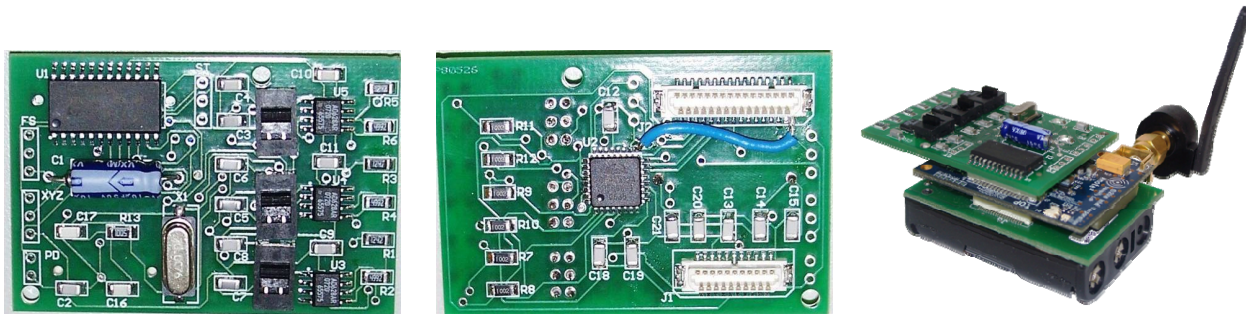

Figure 3. Top view of SHM-A board (left), bottom view of SHM-A board (middle) and SHM-A board stacked on Imote2 and battery board (right).

3.2 Analog accelerometer

Advances in IC technology and the fabrication of Micro-Electro-Mechanical Systems (MEMS) have led to the development of low-cost, high-sensitivity accelerometers. The primary market for MEMS accelerometers in the last 30 years has been in the automotive industry, first for crash testing and more recently for the deployment of airbags; the demand for such sensors for these and a growing number of other applications has led to improved performance and lower cost.[11] Kurata, et. al.[12] summarized the performance of several MEMS accelerometers in the context of SHM applications and ultimately selected the LIS3L02AS4 analog accelerometer manufactured by ST Microelectronics as the best option. The LISL302AS4 is a capacitive-type MEMS accelerometer with DC to 1500 Hz measurement range.[13] Though MEMS accelerometers are available with lower noise levels, the ST Micro accelerometer offers an excellent price/performance ratio. In addition, it offers 3-axes of acceleration on one chip. For these reasons, this accelerometer was selected for the SHM-A sensor board. The specifications for the LIS3L02AS4 accelerometer are given in Table 3. If lower noise characteristics are required for a specific application, a higher-cost accelerometer (such as the Silicon Design SD1221[14] or the Si-Flex SF1500S[15]) could be incorporated readily into the board design.

Table 3. LIS3L02AS4 accelerometer specifications.[13]

Parameter	Value
Axes	3
Measurement Range	±2 g
Resolution	0.66 V/g
Power Supply	2.4 V to 3.6 V
Noise Density	50 μg/√Hz
Temperature Range	-40 to 85˚C
Supply Current	0.85 mA

A design limitation of the ST Micro accelerometer is that it has a high output impedance with a large margin of error in the specified resistor value. Special care must be taken to compensate for the high output impedance and avoid the introduction of error into the output signal. These measures will be discussed in the following sections.

3.3 Low-pass filter

An internal resistor on the LIS3L02AS4 accelerometer is in series with an external capacitor to form a single-pole low-pass RC filter. The value of the internal resistor (R_{source}) is 110 kΩ (±20%). According to the LIS3L02AS4 specifications, the minimum capacitor value that can be used corresponds to a cutoff frequency of approximately 1500 Hz.[13] The cutoff frequency of the filter is defined by the 3 dB roll-off point. This type of filter is not ideal as an anti-aliasing filter, because of its very slow roll-off (6 dB per octave) and non-linear phase distortion. In addition, the accuracy of the amplitude and phase response is subject to the accuracy of the series resistor and capacitor which comprise the filter. The potential error in the accelerometer's internal resistor (±20%) must be addressed to avoid error in the signal amplitude and phase over the bandwidth of interest. Assuming that the capacitor is known precisely, the variation in the resistance can result in a variation in the cutoff frequency which can range from -17% to +25% of the nominal value. The potential phase mismatch between channels at the cutoff frequency can be as high 11.5 degrees.

Figure 4(a) shows the attenuation over a 100 Hz bandwidth associated with three different cutoff frequencies, and Figure 4(b) shows the phase responses of the filter. Figure 4(c) shows the maximum potential phase mismatch between measurement channels for three different cutoff frequencies which could result from the error in the accelerometer's internal resistor. The maximum mismatch at 100 Hz for the 500 Hz nominal cutoff frequency is 4.9 degrees while the maximum mismatch at 100 Hz for the 1500 Hz cutoff frequency is 0.5 degrees.
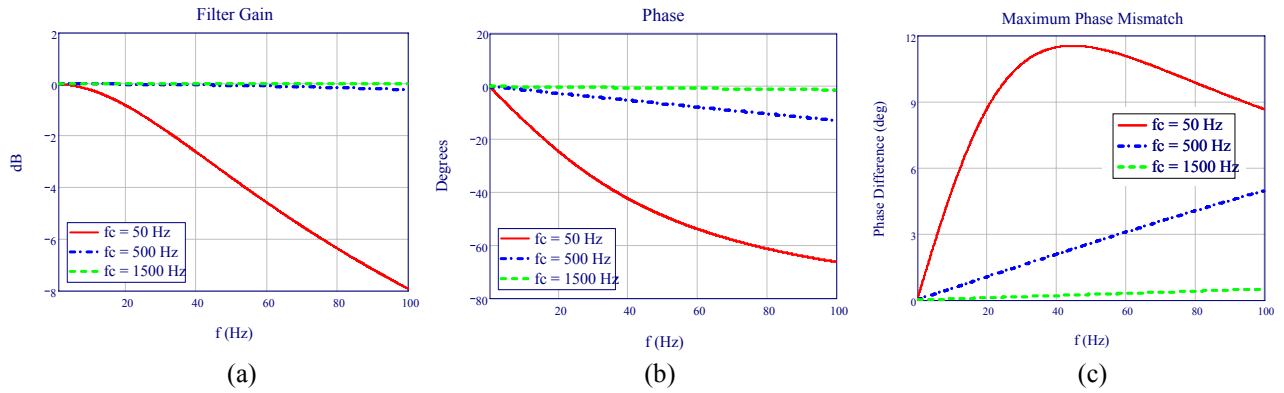

(a) (b) (c)

Figure 4. (a) Single-pole RC filter transfer function, (b) phase response and (c) maximum phase mismatch due to errors in the accelerometer's internal resistor.

To minimize phase and amplitude errors, the highest possible cutoff frequency should be selected for accelerometer. The current SHM-A board configuration allows the user to select between the 50 Hz and the 500 Hz cutoff frequency. Future board revisions will eliminate the switches and fix the cutoff frequency to the highest possible value (1500 Hz). Methods for addressing aliasing will be discussed in Section 3.5.

3.4 Gain difference amplifier

A gain difference amplifier (AD628[16]) follows the accelerometer and low-pass filter (see Figure 2) to compensate for the high output impedance of the accelerometer. A high output impedance (R_{source}) can be problematic if the device that the output signal feeds into has a much lower input impedance (R_{load}) because the signal is attenuated in the following way:

$$V_{load} = V_{source} \frac{R_{load}}{R_{load} + R_{source}} \tag{1}$$

where V_{source} is the signal from the accelerometer and V_{load} is the attenuated signal. The output impendence of the accelerometer is 110 kΩ while the input impedance of the subsequent ADC is 10 kΩ. Without the amplifier, the amplitude of the resulting signal would be less than 10 percent of the original signal. The input impedance of the amplifier is 100 kΩ which results in the accelerometer signal being approximately cut in half.

3.5 Quickfilter ADC

The key component of the SHM-A board is the Quickfilter QF4A512 Programmable Signal Conditioner.[17] The QF4A512 employs a versatile 4-channel, 16-bit resolution ADC. Each channel has a selectable gain (up to 8x), an analog anti-aliasing filter with a 500 kHz cutoff frequency, individually selectable sampling frequencies and individually programmable digital FIR filters (up to 512 filter coefficients). A block diagram of the QF4A512 is shown in Figure 5.
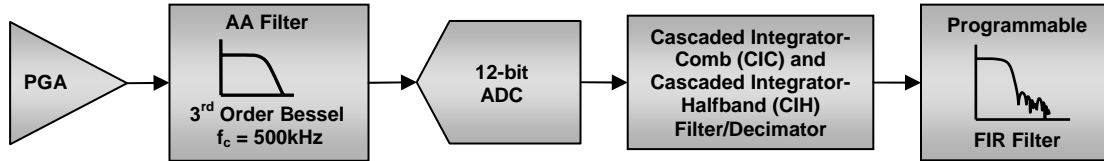

Figure 5. Block diagram for Quickfilter Programmable Signal Conditioner.

The QF4A512 performs oversampling, filtering, and decimation to achieve two purposes in the digitization of the measured signal. The first purpose of oversampling is to improve the resolution of the output by decreasing the noise from quantization error. The resolution of the ADC dictates the smallest measurable increment that can be resolved. Quantization introduces a constant level of noise energy which is uniformly distributed over the measured bandwidth. The higher the sampling frequency, the wider the frequency range over which the noise energy is distributed. Because the energy of the noise is constant, increasing the Nyquist frequency lowers the amplitude of the noise. When a digital decimation filter is applied to the oversampled signal, the noise energy above the new Nyquist frequency is eliminated, thereby improving the resolution of the signal. A 4-times oversampling rate lowers the quantization noise floor by 6 dB or the equivalent of achieving one additional bit in resolution.

The QF4A512 provides variable anti-aliasing filters by following the unaliased, oversampled signal with digital filtering and decimation. The analog anti-aliasing filters are 3rd order Bessel filters with a cutoff frequency of 500 kHz. The digital decimation filters are Cascaded-Integrator-Comb (CIC) filters, working in combination with the Cascaded-Integrator Halfband (CIH) filters to ensure that the integrity of the signal is maintained upon decimation to the final user-specified sampling frequency. This combination of filters provides excellent amplitude response and while preserving a linear phase response.[18] This method of oversampling, filtering and decimation to remove aliasing is common for PC-based analyzer systems such as those offered by Siglab.[19]

The gain, sampling rate and user designed FIR filters are all set with the use of software provided by Quickfilter Technologies, Inc.[20] The user first selects the desired FIR filter type. The available filter types are Basic Parks-McClellan, Window Sync Blackman, and Window Sync Blackman-Harris with low-pass, high-pass, band-pass and band-stop options. The user then selects the final sampling rate and filter characteristics in the *FIR Specification Editor*

as shown in a screen shot in Figure 5. The analog gain is then selected and the filter is assigned to the measurement channels. Finally, the results of the filter design and configuration are exported to a header file which is included when the sensing application is loaded onto the Imote2.
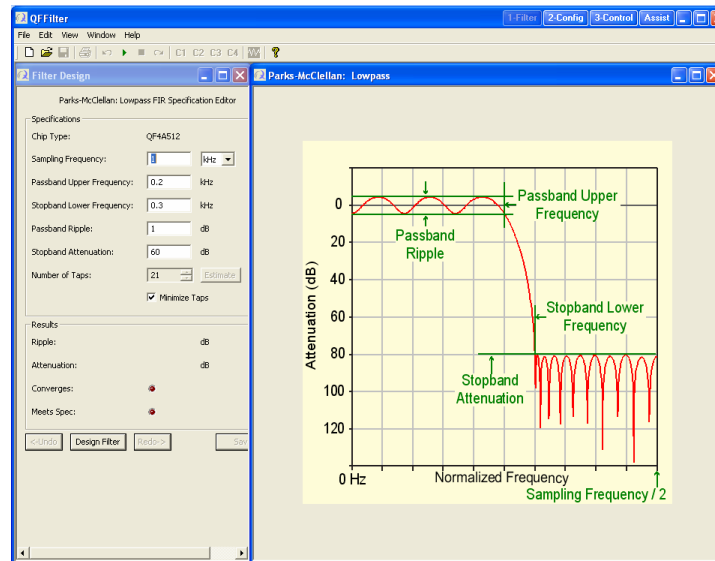

Figure 6. Screen shot of Quickfilter FIR filter design software interface

3.6 Clock components

The master clock of the QF4A512 uses an external signal provided by a surface mounted 20 MHz crystal (Citizen HCM-49[21]). All internal clocks are derived from the master clock through the use of dividers. The clock used to drive the ADC has a default frequency of 100 MHz and the system clock, which runs the FIR filters, has a default frequency of 200 MHz[14]. The accuracy in the effective sampling rate of the output signal depends on the accuracy of the external crystal which is specified as ±30 ppm (0.003%). The processor clock on the Imote2 runs at 3.25 MHz, which is assumed to be accurate, although it could also be a source of sampling rate error.[3]

3.7 Software development

A software driver for the SHM-A board was developed in TinyOS. The purpose of the driver is to control the functions of the QF4A512 such as loading the filter coefficients, allocating memory, timestamping, writing data, etc. The driver was adapted from driver code provided by Intel and implemented for the SHM-A board.

The driver first initializes the ADC and then triggers the sampling to start. One limitation of the driver which is derived from an inherent limitation of TinyOS is the inability to accurately control the time delay between the command to begin sampling and the actual start of sampling. During sampling, the samples are released from the QF4A512 and written to the Imote2 buffers as two-byte integers (16-bit). Timestamping occurs at multiples of the sampling time. If timestamping is requested, the timestamps are written with the ADC data at this lower specified frequency (e.g. every 10 samples).

4. SENSOR BOARD VALIDATION

4.1 Calibration testing

Tests were conducted to calibrate each channel of the accelerometer. The SHM-A board mounted on an Imote2 was placed on an accelerometer calibration frame which ensured a level measurement surface. Measurements were taken with the board oriented so that signals corresponding to –1 g, 0 g and +1 g were measured for each of the measurement axes. The results provided the necessary calibration constants which can be directly implemented in the sensing application.

The SHM-A board was also tested on a bench-scale shake table[22] against a wired reference sensor (Figure 7). The reference sensor is a capacitive accelerometer (PCB Model 3701G3FA3G[23]) with 1 V/g sensitivity and DC to 150 Hz measurement range. Several types of excitations were used to test the performance of the sensor board. Because lower frequency performance of the sensor is important for civil structures, focus was placed on the 0 to 20 Hz range. To compensate for the limitations of the shake table in the lower frequency range, a "shaped" band-limited white noise with a 10 Hz cutoff frequency was used. The results given in Figure 8(a) show excellent agreement between the wired sensor and the SHM-A board in the time and frequency domain. Additionally, the higher frequency range was excited by a band-limited white noise with a 50 Hz cutoff frequency as shown in Figure 8(b).
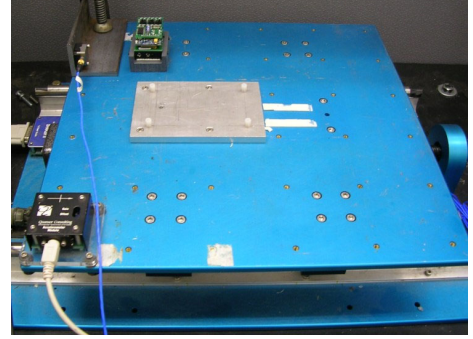

Figure 7. Reference sensor and SHM-A board with Imote2 mounted on a bench-scale shake table for calibration testing.
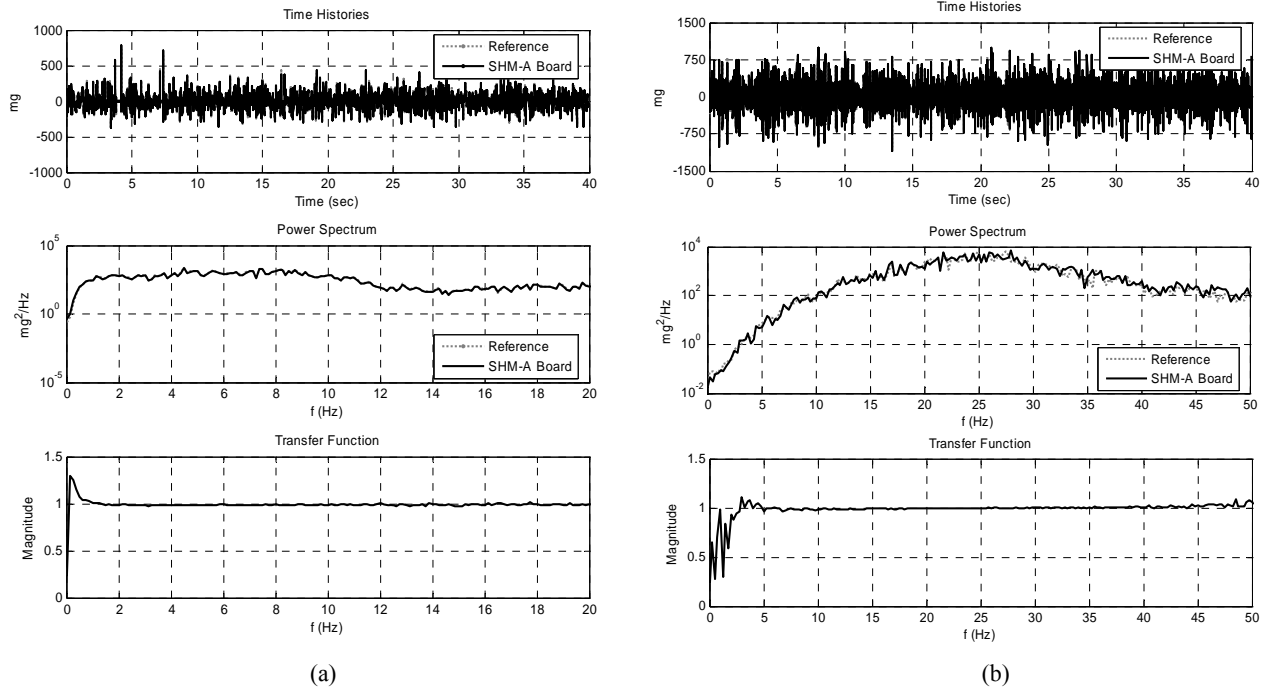

| | |
| (a) | (b) |

Figure 8. Time history and power spectrum plots of shake table tests for (a) a "shaped" 10 Hz band-limited white noise excitation and (b) a 50 Hz band-limited white noise excitation.

4.2 Noise and resolution

Tests were conducted to quantify the noise floor and resolution of the SHM-A sensor board. The Quickfilter ADC has a nominal resolution of 16 bits.[14] The acceleration range of the ST Micro accelerometer is ±2 g at a sensitivity of 0.66

V/g and a zero-g offset equivalent to half of the supply voltage. The gain difference amplifier results in a halving of the output of the accelerometer; therefore the full range is 2g*0.66 V/g = 1.33 V. Using a selectable gain on the Quickfilter ADC of 8, results in a nominal resolution of 0.163 mg. However, the signal-to-noise ratio of the ADC, resulting from noise within the device, is given as 81 dB which corresponds to 13.2 effective number of bits (ENOB). As discussed previously, oversampling can result in an increase in the number of bits achieved beyond those realized in hardware.

Inherent noise is present in the accelerometer and other components, in addition to the noise resulting from the ADC quantization. The noise floor of the accelerometer is given as 50 μg/√Hz[13]. Over a 128 Hz bandwidth this corresponds to an RMS noise level of 0.57 mg and is therefore expected to be the controlling factor in the overall noise floor of the sensor.

The actual RMS noise level of the accelerometer was determined by conducting still tests with the SHM-A board resting on a rubber-backed aluminum plate on placed on the concrete strong floor of the Smart Structures Technology Laboratory in the basement of Newmark Civil Engineering Laboratory. The measured values for all three channels was determined to be approximately 1.3 mg over a bandwidth of 128 Hz which is equivalent to 11.6 ENOB or a noise floor of 71.6 dB. The noise floor of the acceleration output can be improved in a few ways. The first is to precede the difference gain amplifier with an operational amplifier to prevent the signal from being cut in half prior to the QF4A512. As previously mentioned, a different accelerometer with lower noise characteristics could be used which would be expected to result in lower noise levels in the final output.

4.3 Clock accuracy

The sampling rate accuracy of the QF4A512 was tested to determine how closely the actual sampling rate matches the requested sampling rate and to observe any fluctuation in the sampling rate over time. The tests were conducted by requesting a timestamp corresponding to every 10th data point at a nominal sampling rate of 1000.32 Hz. Taking the difference between the consecutive timestamps gives a picture of how the sampling rate fluctuates in time as shown in Figure 9. The mean value divided by 10 yields the observed sampling rate. The actual sampling rate was determined to be 1000.44 Hz corresponding to an error of 0.012%. By dividing the time difference between each timestamp by 10 the estimated fluctuation in the sampling rate has an RMS value of 0.11 μs or 0.011%. The observed sample rate fluctuates about the mean value and therefore is not expected to introduce significant error over time.
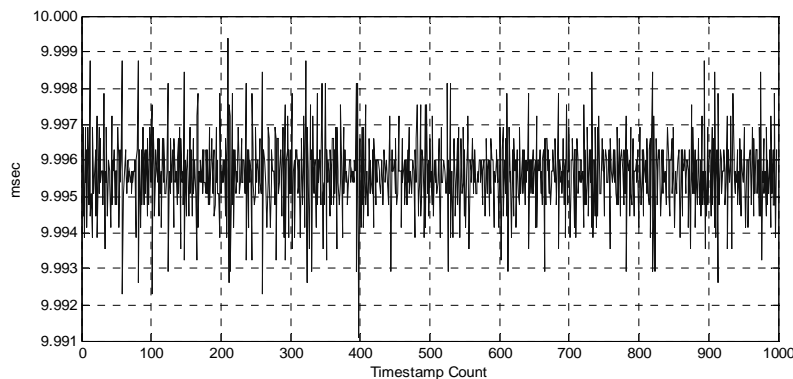

Figure 9. Time elapsed between timestamps taken every 10 samples at a sampling rate of 1000.32 Hz.

During initial clock-rate testing, an attempt was made to timestamp each sample when sampling at 1000 Hz. This rate timestamping proved to be too demanding a task to perform in conjunction with the data acquisition and actually introduced error in the sampling rate. To minimize this effect, timestamps were limited to every 10th point for the purpose of testing. Based on these observations, some of the sample rate variation that appears in Figure 9 may be the result of the timestamping itself.

The results of the clock accuracy tests show that while there is some observed error in the sampling rate, it is quite small and is not expected to compromise efforts to achieve synchronized sensing. In comparison to the observed sample rate error of 10% and a non-zero mean sample rate fluctuation of 0.1% of the *Basic Sensor Board,*[7] the sampling rate accuracy of the SHM-A board is a significant improvement.`

4.4 Power consumption

The specified supply currents and typical supply voltages for each of the components or the SHM-A sensor board are given in Table 4. The values shown for the QF4A512 are assuming three-channel operation at a 1000 Hz sampling rate. The QF4A512 utilizes both 3.3 V and a 1.8 V power supplies for various functions within the chip, both supplied by the Imote2. According to the specifications, the power consumption of the QF4A512 is a function of the number of active channels and the sampling rate; the number of FIR filter coefficients have negligible effect.[24]

Table 4. Specified power consumption of SHM-A components.[24]

Component	Active Current (mA)	Supply Voltage (V)	Power (mW)
Accelerometer (LIS3L02AS4)	0.85	3.3	2.8
Gain Difference Amplifier (AD628)	1.6	5.0	8.0
QF4A512 PGA	12.7	3.3	41.9
QF4A512 anti-aliasing filters, ADC, clocks	72.8	1.8	131.0
QF4A512 FIR filters	6.8	1.8	12.3
QF4A512 SPI operation	0.06	3.3	0.2
Total Power			196.2

Tests were conducted to measure the actual power consumption of the SHM-A board while data acquisition is taking place. A 4.5 V DC power source was connected to the battery board to represent the nominal voltage from 3-AAA batteries. The Imote2 was turned on and the current draw from the Imote2 and battery board was measured. The sensor board was then attached to the Imote2 and the current was measured again. Data acquisition was initiated and the current was observed during sensing. In this way, the incremental power consumption of the SHM-A board during sensing was estimated. The results are shown in Table 5 for two different sampling rates with either one active channel or three active channels.

Table 5. Estimated SHM-A Power consumption when powered by 4.5V DC power source.

Sampling Rate (Hz)	Active Channels	Imote2 On – No Sensor Board Attached		Imote2 + SHM-A Board – Inactive		Imote2 + SHM-A Board – Sensing	
		Current (mA)	Power (mW)	Current (mA)	Power (mW)	Current (mA)	Power (mW)
500	1					110	495
500	3	60	270	70	315	155	698
1000	1					110	495
1000	3					155	698

The inactive SHM-A board attached to the Imote2 requires in an additional 10 mA of current. In the data acquisition mode the Imote2 and SHM-A board acting together require approximately 500 mW for one active channel and 700 mW for three active channels. No difference was observed between the two sampling rates tested. During data acquisition, the Imote2's operating frequency is switched to 104 MHz which results in increased power consumption.

5. FUTURE WORK

The next phase in SHM sensor development for the Imote2 is to incorporate strain measurement capabilities. Preliminary studies have shown that combining acceleration and strain measurements results in more effective damage detection.[25],[26] This multi-scale SHM sensor board will utilize the QF4A512 for signal conditioning of the strain measurements. QF4A512s can be cascaded to ensure synchronized sensing between multiple chips.[27] In addition, the sensor board will incorporate temperature, humidity, and light sensors. The temperature sensor will allow the signals from the sensors to be calibrated to account for temperature changes as well as give more insight to the structural response under varying environmental conditions.

A full-scale implementation of an Imote2 sensor network is planned for a historic truss bridge in Mahomet, Illinois (Figure 10). Critical network implementation issues, such as communication range evaluation, multi-hop communication implementation, environmental hardening, network bandwidth optimization, and fault tolerance will be addressed.

Figure 10. Historic bridge over the Sangamon River in Mahomet, Illinois.

6. CONCLUSION

This paper has described the features of the Imote2 which make it well-suited to the demands of SHM applications. The limitations of the currently available Imote2 sensor board have been reviewed, and the need for more versatile signal processing has been discussed. The design and validation of the Imote2 SHM-A sensor board has with flexible signal processing capabilities has been presented. The SHM-A board provides user-selectable anti-aliasing filters with variable cutoff frequencies, while maintaining high sampling rate accuracy. Future versions of the SHM-A board are planned that will improve the signal output quality, expand sensing capabilities, and streamline the design.

7. ACKNOLEDGEMENT

8. REFERENCES

[1] Spencer Jr., B. F., Ruiz-Sandoval, M and Kurata, N. "Smart Sensing Technology: Opportunities and Challenges" Structural Control and Health Monitoring 11, 349–368 (2004).
[2] Nagayama, T. Sim, S. H., Miyamori, Y., Spencer Jr., B. F. "Issues in structural health monitoring employing smart sensors," Smart Structures and Systems, (accepted) (2007).
[3] Nagayama, T. and Spencer Jr., B. F., "Structural health monitoring using smart sensors," NSEL Report, Series 001, http://hdl.handle.net/2142/3521 (2007).
[4] Crossbow Technology, Inc, "MICA2 Wireless Measurement System," San Jose, CA (2007).
[5] Crossbow Technology, Inc., ITS400, Imote2 Basic Sensor Board, San Jose, CA, (2007).
[6] Intel Corporation Research, Intel Mote2 Overview, Version 3.0, Santa Clara, CA (2005).

[7] Nagayama, T., Rice, J. A., and Spencer Jr., B. F. "Efficacy of Intel's Imote2 wireless sensor platform for structural health monitoring applications," Proc. Asia-Pacific Workshop on Structural health Monitoring, Yokohama, Japan (2006).

[8] TinyOS, http://www.tinyos.net, (2006).

[9] STMicroelectronics, "LIS3L02DQ MEMS Inertial Sensor," Geneva, Switzerland (2005).

[10] STMicroelectronics, "AN2041 Application Note," Geneva, Switzerland, (2005).

[11] Walter, P.L., "The History of the Accelerometer, 1920s-1996 – Prologue and Epilogue, 2006," Sound and Vibration 4(11), 84-90, Acoustical Publications (2007).

[12] Kurata, N., Saruwatari, S. and Morikawa, H., "Ubiquitous Structural Monitoring using Wireless Sensor Networks," Proc. ISPACS (2006).

[13] STMicroelectronics, "LIS3L02AS4 MEMS Inertial Sensor," Geneva, Switzerland (2005).

[14] Silicon Designs, Inc., "Model 1221 Low Noise Analog Accelerometer," Issaquah, WA (2007).

[15] Colibrys Inc., "Si-Flex SF1500S Accelerometer," Neuchatel, Switzerland (2007).

[16] Analog Devices, Inc., "High Common-Mode Voltage, Gain Difference Amplifier AD628," Norwood, MA (2007).

[17] Quickfilter Technologies, Inc., "QF4A512 4-Channel Programmable Signal Conditioner," Allen, TX (2007).

[18] Hogenauer, E. B. "An economical class of digital filters for decimation and interpolation". IEEE Transactions on Acoustics, Speech and Signal Processing 29(2), 155-162 (1981).

[19] Spectral Dynamics, Inc., San Jose, CA.

[20] Quickfilter Technologies, Inc., Quickfilter Pro Software, Allen, TX (2007).

[21] Citizen Component Sales Div., HCM49, Torrance, CA (2007).

[22] Quanser Inc., "Quanser Shake Table II, Product Information Sheet," Ontario, Canada (2006).

[23] PCB Piezotronics Inc. "Model 3701G3FA3G Capacative Accelerometer Installation and Operating Manual," Depew, NY (2007).

[24] Quickfilter Technologies, Inc., "QFAN006 Application Note: Power Optimization for the QF4A512 Programmable Signal Conditioner," Allen, TX (2005).

[25] Kijewski-Correa, T., Haenggi. M., and Antsaklis, P., "Multi-scale wireless sensor networks for structural health monitoring." Proc., 17th Analysis &. Computation Specialty Conference, ASCE St. Louis, MO (2006).

[26] Sim, S. H. and Spencer Jr., B. F., "Multi-scale sensing for structural health monitoring", Proc. World Forum on Smart Materials and Smart Structures Technology, Chongqing, China (2007).

[27] Quickfilter Technologies, Inc., "QFAN020 Application Note: Synchronized Sampling Using Multiple QF4A512 Programmable Signal Converters," Allen TX (2007).